PHYSICAL REVIEW B VOLUME 52, NUMBER 24 15 DECEMBER 1995-II

Low-temperature electron mobility studied by cyclotron resonance in ultrapure GaAs crystals

M. Kozhevnikov, B. M. Ashkinadze, E. Cohen, and Arza Ron
Solid State Institute, Technion-Israel Institute of Technology, Haifa 32000, Israel
(Received 18 August 1995)

We report on a systematic study of the electron scattering processes in ultrapure GaAs crystals over the temperature range 1.6–100 K by using the classical cyclotron resonance (CR) for a low density of photogenerated electrons ($n_e \sim 10^{10}$ cm^{-3}). The highest electron mobility extracted from the CR data is 2.2×10^6 cm^2/V sec at $T=1.6$ K. The electron scattering due to the acoustic-phonon piezoelectric potential is found to be the main intrinsic electron-phonon scattering mechanism in the temperature range $1.6<T<30$ K. Electron scattering by neutral impurities is shown to be significant even in these ultrapure GaAs crystals (unlike Ge and Si). The acoustic-phonon piezoelectric and deformation-potential coefficients as well as the impurity concentrations ($\sim10^{13}$ cm^{-3}) were obtained from the analysis of the electron-scattering-rate dependence on temperature. A CR line narrowing is observed under increasing microwave power and is interpreted as due to a decrease in the acoustic-phonon piezoelectric scattering efficiency with electron heating. The electron effective mass determined from the CR magnetic field applied along [001] is $m^*=(0.0662\pm0.0002)m_0$.

I. INTRODUCTION

Carrier-scattering processes by imperfections play a crucial role in the transport phenomena in semiconductors. For Ge and Si crystals there are detailed experiments and a good theoretical understanding of the different scattering mechanisms for electrons and holes.[1,2]

Despite the great progress in the growth and application of GaAs, the intrinsic electron-phonon scattering mechanisms at low temperatures could not be investigated experimentally, since the scattering of electrons by residual impurities usually governs the mobility for $T<50$ K.

One of the most powerful methods for the study of carrier-scattering mechanisms in semiconductors is the classical cyclotron resonance (CR).[2] In GaAs, CR was studied only in the quantum limit,[3] where a high magnetic field and radiation frequency enabled the study of low-mobility GaAs samples. However, the scattering processes are different from those expected in the classical limit.[4]

Ultrapure epitaxial GaAs layers with a shallow impurity concentration in the range $10^{12}-10^{13}$ cm^{-3} can be grown by vapor-phase epitaxy (VPE) in a chlorine system.[5] These samples exhibit a strong polariton photoluminescence[6] (PL) and a long electron momentum relaxation time, resulting in an electron mobility of up to 3×10^6 cm^2/V sec at 2 K.[7] The availability of such ultrapure samples enables the use of classical CR for studying the intrinsic electron-scattering processes at low temperatures.

The expression for the microwave (MW) power absorption of linearly polarized radiation with frequency ω and electric-field strength E due to an electron rotating in the magnetic field B is given in the classical case by[8]

$$P(\omega)=\sigma_0|E|^2\frac{1+(\omega^2+\omega_c^2)\tau^2}{[1+(\omega^2-\omega_c^2)\tau^2]^2+4\omega_c^2\tau^2} . \quad (1)$$

Here $\sigma_0=ne^2\tau/m^*$ is the dc conductivity, τ is momentum relaxation time, $\omega_c=eB/m^*c$ is the cyclotron frequency, and m^* is the electron effective mass. If $\omega_c\tau>1$, the resonance occurs at $\omega=\omega_c$ and τ can be obtained from the full width of the CR line at half its maximum, ΔB, by the expression

$$\omega_c\tau=2B_r/\Delta B , \quad (2)$$

where B_r is the resonance magnetic field. τ^{-1} is the total momentum relaxation rate and it is expressed as a sum of the inverse-relaxation times for each of the scattering mechanisms.

The momentum relaxation time, which is derived from the CR line shape, is the same as that determined from dc measurements, as long as the magnetic field is weak and the cyclotron radius is large compared with the force range of the scattering center.[2] This is the case of the classical limit ($\hbar\omega<kT$), wherein the scattering processes are not affected by the magnetic field.

This paper presents an experimental study of the classical electron CR in photoexcited, ultrapure GaAs samples. For the MW frequency used (35.6 GHz), the CR occurs at a magnetic field of ~0.085 T. Under these conditions, electron-scattering processes can be studied in ultrapure GaAs crystals in the temperature range 1.6–100 K. We compare the extracted low-temperature mobility values for different GaAs samples grown by vapor-phase epitaxy (VPE) and molecular-beam epitaxy (MBE) techniques. The analysis of the temperature-dependent mobility yields the relative significance of electron-phonon and electron-impurity scattering processes.

The paper is laid out as follows: In Sec. II, the experimental setup, the samples used, and the experimental results are presented. An analysis and a comparison of the theoretical predictions with the experimental results are given in Sec. III. In Sec. IV, we discuss our findings and conclude the paper.

0163-1829/95/52(24)/17165(7)/$06.00 52 17 165 ©1995 The American Physical Society

II. EXPERIMENTAL PROCEDURE AND RESULTS

Ultrapure samples grown by the VPE and MBE methods with layer widths 5–10 μm are studied. A detailed analysis will be presented for three typical GaAs samples denoted A (VPE), B (VPE), and C (MBE). They differ in the background impurity concentrations. The sample is placed at the antinode of the MW electric field in an 8-mm waveguide which is short circuited by a plunger at one end. The MW radiation reflected from the plunger was directed onto a diode detector by a circulator. The waveguide is immersed either in liquid He or in cold He gas so that the temperature is varied in the range $T=1.6-100$ K. The sample is illuminated by either above-gap or below-gap laser light (from a He-Ne or a tunable dye laser) through a pinhole in the waveguide. The light intensity I_L was low so that the photogenerated free-electron density was of the order of $n_e \leq 10^{10}$ cm^{-3} at a photoexcitation level of 10 mW/cm^2. The excitation was modulated at a frequency varying in the range 10–400 Hz.

A stabilized 35.6-GHz Gunn diode was used as the MW source. An electrically controlled attenuator allowed us to vary the incident MW power, P_{MW}, continuously so that the power incident on the sample was in the range $10^{-4}-10$ mW. The MW radiation measured by the diode detector was modulated by the photoexcitation of the sample and the modulation signal was proportional to the MW power absorbed by the photoexcited free electrons. The external dc magnetic field **B** was applied parallel to the [001] direction and was swept over the range 0–0.25 T. The MW electric field was perpendicular to **B**, and the absorbed MW power was measured as a function of scanned magnetic field. The aforementioned I_L and P_{MW} values were set at the minimal possible values so that they do not affect the CR line shape.

The CR line shape has been measured under photoexcitation by a dye laser at the exciton resonance, $E_L=1.515$ eV, and also by a He-Ne laser at $E_L=1.96$ eV. Typical CR traces at various temperatures are presented in Fig. 1, all normalized to the same peak value (sample A, $E_L=1.96$ eV). Similar traces are observed for the other samples and for $E_L=1.515$ eV. The CR line is broadened as the lattice temperature T increases. The temperature dependence of the inverse relaxation time, $\tau^{-1}(T)$, extracted from the CR lines [by using Eq. (1)], is shown in Fig. 2 for the three samples. The $\tau^{-1}(T)$ curves are different for each GaAs sample in the range $1.6<T\leq 30$ K (due to different impurity concentrations), but are the same for $T>30$ K.

We observed that the CR line is modified as P_{MW} increases. The CR linewidth first decreases with increasing P_{MW} (for example, up to $P_{MW}\sim 1$ μW for sample A) and then broadens again with further power increase. This behavior of the CR line shape for sample A is demonstrated in the inset of Fig. 3. A similar behavior is also observed for the other samples having a lower mobility, but the range of P_{MW} where the CR linewidth varies is different, as shown in Fig. 3 for two samples. The CR linewidth decrease in the terms of τ^{-1} is also marked by the arrows in Fig. 2 for all three samples (at $T\sim 2$ K).

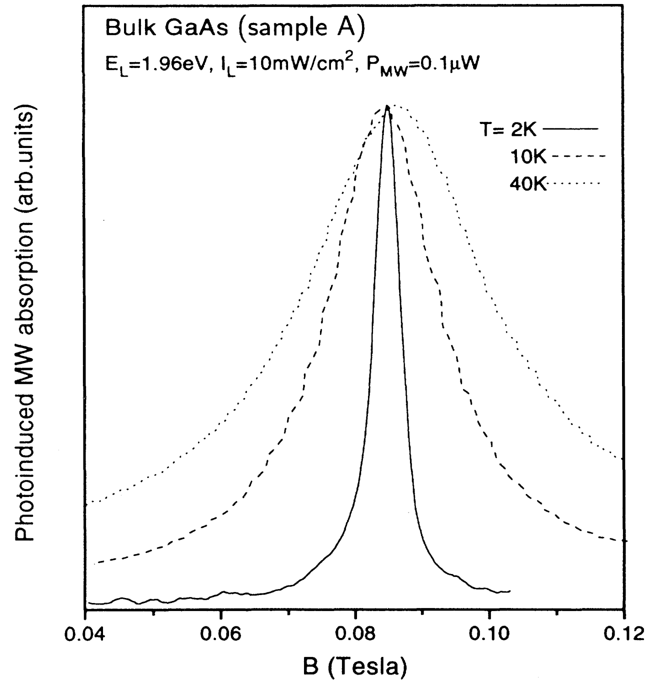

FIG. 1. Photoinduced CR traces of ultrapure GaAs observed at three lattice temperatures.

Figure 4 shows the photoluminescence spectra in the exciton region. Since the measured PL intensity in the range of donor-acceptor pair recombination (not shown) is 200 times weaker than that of the excitons for all three samples, the impurity concentration is genuinely ultralow.[6]

Several authors[9] have extracted the momentum relaxation time from the optically detected CR (ODCR). Using

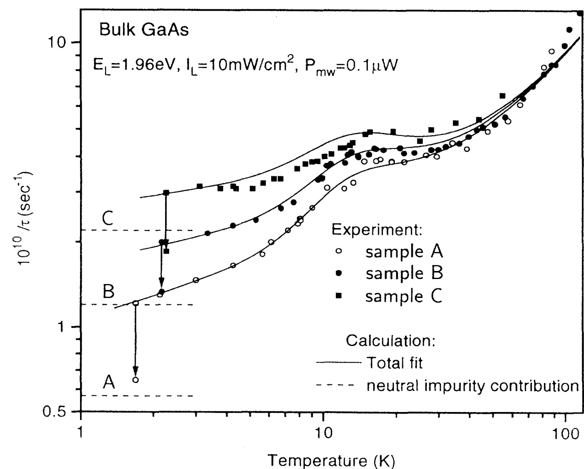

FIG. 2. The temperature dependence of the electron inverse relaxation time for three samples. The values were obtained from CR traces (as in Fig. 1) by using Eq. (1). The model-fitting [Eq. (3)] curves are shown by solid lines. The decrease of τ^{-1} that is due to electron heating (by increased P_{MW} at $T\sim 2$ K is marked by the arrows.

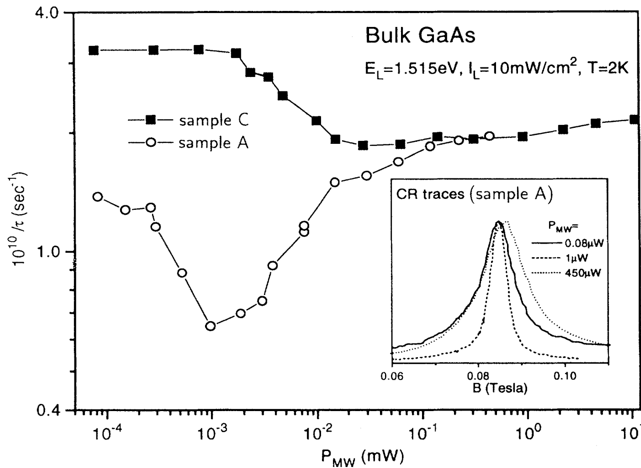

FIG. 3. The dependence of τ^{-1} on the microwave power. The inset shows the CR line shape traces for sample A at three different P_{MW} values.

this method, the photoluminescence quenching under high MW power is measured as a function of the magnetic field. Typical ODCR traces are shown in Figs. 5(a) (for sample A) and 5(b) (for sample C), monitored at the polariton line (1.515 eV) under photoexcitation at $E_L = 1.96$ eV. For comparison, the CR line shapes are also shown. It is seen that the line shape of the ODCR is different

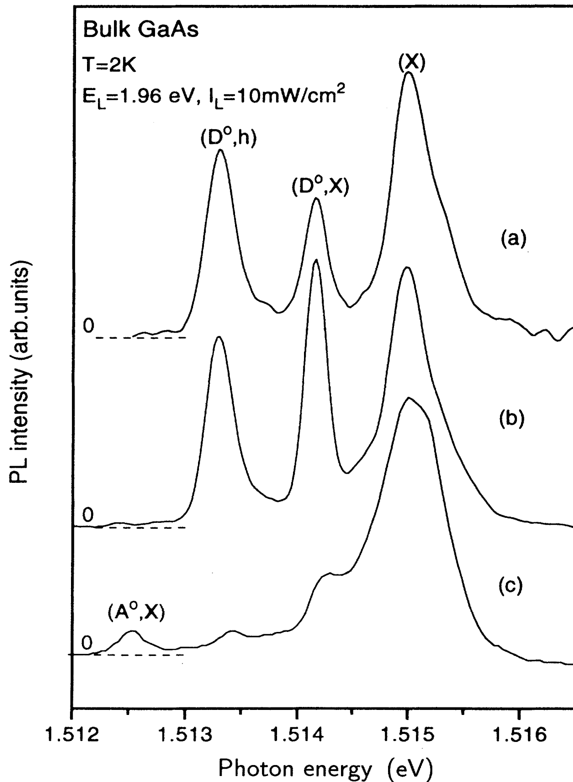

FIG. 4. The photoluminescence spectra in the exciton region (observed with $P_{MW} = 0$) for samples (a) A, (b) B, and (c) C.

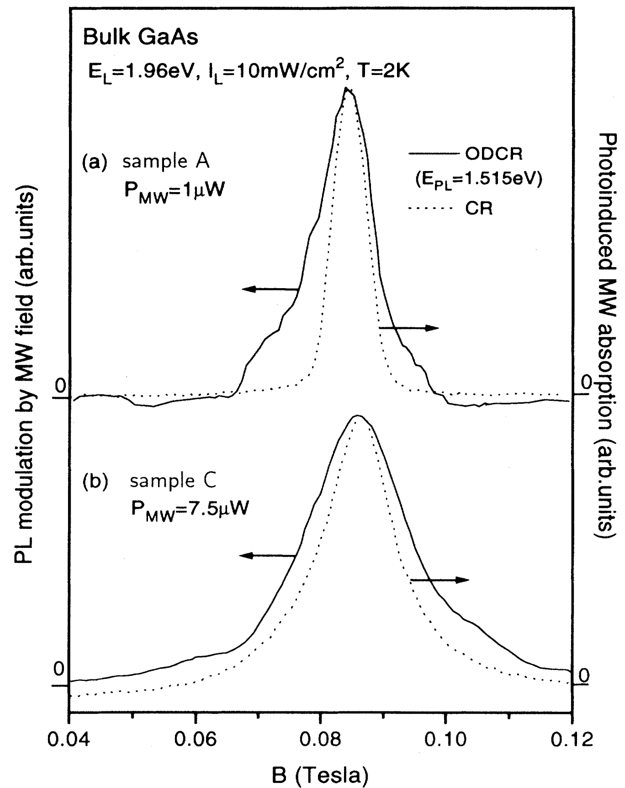

FIG. 5. A comparison between the ODCR and CR traces. The ODCR data were observed monitoring the exciton-polariton PL line (1.515 eV).

from that of the CR when both are observed under the same conditions (temperature, MW power, and photoexcitation intensity).

III. ANALYSIS

So far, a systematic study of free-electron scattering processes was carried out in GaAs by means of CR measurements, only in the quantum limit ($kT < \hbar\omega$).[3] In this case, the efficiency of electron scattering by impurities is reduced[4] and, therefore, the electron-phonon scattering mechanisms could be studied in samples with impurity concentration of $\sim 10^{15}$ cm^{-3}.[3] The experimental results indicated that the electron-phonon scattering rates (measured under magnetic fields up to 10 T) could be explained by the classical limit expressions ($B \to 0$). This is in spite of the fact that the theoretical prediction in the quantum limit differs significantly from that for the classical limit.[4] The electron-scattering mechanisms at $B \to 0$ (classical limit) have not been studied yet because of the unavailability of very pure samples.

Our present studies extend the electron CR in ultrapure GaAs to the classical limit. This allows us to obtain the relative contributions of the main electron-scattering mechanisms in GaAs crystals in the temperature range 2–100 K. The model used to fit the experimental results assumes that the total momentum relaxation rate is given by a sum of the inverse-relaxation times for each contrib-

uting electron-scattering mechanism,

$$\tau^{-1}(T)=\tau_{ni}^{-1}+\tau_{ii}^{-1}+\tau_{pe}^{-1}+\tau_{dp}^{-1} . \quad (3)$$

Here τ_{ni}^{-1} and τ_{ii}^{-1} are the electron scattering rates by neutral and ionized impurities, respectively; τ_{pe}^{-1} and τ_{dp}^{-1} are the acoustic-phonon scattering rates via the piezoelectric and the deformation potentials, respectively. The contribution of the electron scattering by polar optical phonons via the Fröhlich interaction takes over only at the upper edge of our temperature range, and therefore, it was not included in the fitting procedure. The theoretical expressions for each process,[10,11] as well as the parameters extracted from the fitting are summarized in Table I.

The following notation is used in Table I: N_N is the neutral impurity density concentration, N_I is the total concentration of ionized donors and acceptors, T_e is the electron temperature, T is the lattice temperature, ε is the dielectric constant, ε_0 is the permittivity of free space, K^2 is the electromechanical coupling constant, E_1 is the deformation-potential constant, ρ is the crystal density, and s is an averaged velocity of sound.[10]

It is seen from Table I that the neutral impurity scattering rate is temperature independent. The scattering of electrons by singly ionized impurities is described by the Conwell-Weisskopf equation[15] and the inverse relaxation time is proportional to $T^{-3/2}$. For the acoustic-phonon piezoelectric scattering, τ^{-1} is proportional to $T^{1/2}$ and for the acoustic-phonon deformation-potential scattering, to $T^{3/2}$ (at thermodynamic equilibrium, $T=T_e$). Note that the electron temperature may be different from that of the lattice as a result of electron heating by the MW electric field.

At low temperatures ($T\leq 30$ K), the observed values of τ^{-1} are different for the three samples, while at higher temperatures they are essentially equal (Fig. 2). In the temperature range 50–100 K, the experimental dependence is $\tau^{-1}\sim T^{3/2}$ for all three samples and, therefore, it is due to the acoustic-phonon deformation-potential scattering. For $T>100$ K, the τ^{-1} dependence is dominated by the polar optical-phonon scattering.[13] Figure 2 shows that the $\tau^{-1}(T)$ for the purest sample A can be approximated by a $T^{1/2}$ dependence in the range $4\leq T\leq 50$ K, except for the temperature range 10–20 K (it will be discussed below). It means that the main scattering mechanism is due to the acoustic-phonon piezoelectric potential (cf. Table I).

For $T<10$ K, the $\tau^{-1}(T)$ is independent of T for sample C and only weakly so for sample B. Thus, the scattering rate in this temperature range is dominated by neutral-impurity scattering. This can be expected for sparsely compensated crystals with a low impurity content, since under photoexcitation ionized impurities are completely neutralized and the ionization rate is extremely small for $T<10$ K. Then the different τ^{-1} values for each sample reflect the decrease in the impurity concentration. For $T>30$ K, the scattering by impurities is insignificant, and the intrinsic phonon scattering becomes dominant.

In the temperature range 10–20 K, an additional increase of the scattering rate is observed for all three samples. This is due to the fact that as the temperature increases, the neutral impurities are ionized and free-electron scattering by ionized impurities becomes important ($\tau_{ii}\ll\tau_{ni}$). As the temperature increases further, the ionized-impurity contribution decreases as $T^{-3/2}$. We note that a similar, less pronounced scattering-rate increase was observed in the quantum limit case.[3]

TABLE I. Summary of theoretical expressions for each scattering process and the parameters extracted from the fitting procedures.

Type of scattering	τ_i^{-1}	This work	Parameters from references
Acoustic-phonon piezoelectric potential	$\frac{1}{\tau_{pe}}=\frac{3\sqrt{m^* k_B}e^2K^2T}{16\sqrt{2\pi}\hbar^2\varepsilon\varepsilon_0 T_e^{1/2}}$	$1/\tau_{pe}=5\times10^9T^{1/2}$ sec^{-1} ($K^2=3.59\times10^{-3}$)	$1/\tau_{pe}=3.9\times10^9T^{1/2}$ sec^{-1} (12) $1/\tau_{pe}=5.7\times10^9T^{1/2}$ sec^{-1} (13) $K^2=4.4\times10^{-3}$ (14)
Acoustic-phonon deformation potential	$\frac{1}{\tau_{dp}}=\frac{3E_1^2T(m^{*3}k_B^3T_e)^{1/2}}{2\sqrt{2\pi}\hbar^4\rho s^2}$	$1/\tau_{dp}=4\times10^7T^{3/2}$ sec^{-1} ($E_1=7.64$ eV)	$1/\tau_{dp}=2.8\times10^7T^{3/2}$ sec^{-1} ($E_1=7$ eV) (13)
Ionized impurities	$\frac{1}{\tau_{ii}}=\frac{e^4N_I}{128\sqrt{2\pi m^*}(\varepsilon\varepsilon_0)^2(k_BT_e)^{3/2}}\ln\beta$ where $\beta=1+\left[\frac{12\pi\varepsilon\varepsilon_0k_BT_e}{e^2N_I^{1/3}}\right]^2$	$E_i=5.8$ meV $N_D=1.5\times10^{13}$ cm^{-3} (A) 2.2×10^{13} cm^{-3} (B) 3.0×10^{13} cm^{-3} (C)	$E_i=5.8$ meV (3) $E_i=5.30$–5.52 meV (13)
Neutral impurities	$\frac{1}{\tau_{ni}}=aN_N$ where $a=\frac{80\pi\varepsilon\varepsilon_0\hbar^3}{m^{*2}e^2}$	$a=3.8\times10^{-4}$ cm^{3}sec^{-1} (A) $=5.5\times10^{-4}$ cm^{3}sec^{-1} (B) $=7.3\times10^{-4}$ cm^{3}sec^{-1} (C)	$a=3.5\times10^{-4}$ cm^{3}sec^{-1} (10) ($m^*=0.066m_0$, $\varepsilon=12.5$)

The temperature-dependent densities of the ionized and neutral impurities, N_I and $N_N=N_0-N_I$, respectively (N_0 is the total impurity concentration), can be estimated as follows. From the PL data (Fig. 4), we see that the acceptor concentration N_A is very small in all three samples, and hence we assume that $N_0=N_D$, where N_D is the donor concentration. Then, we may write[16]

$$N_I=\frac{N_D}{2\exp\{(\mu-E_D)/k_BT\}+1}\ , \tag{4}$$

where μ is the temperature-dependent Fermi level[16] and E_D is the energy of the 1s donor state. For extremely low photoexcitation intensities, the photoexcited-electron concentration is far less than that of donors, and therefore, the steady-state Fermi level is approximated by its equilibrium value. Setting this value into Eq. (3), we obtain the expression for the ionized-donor concentration,

$$N_I=\frac{2N_D}{1+(1+8N_D/N_C\exp\{E_i/k_BT\})^{1/2}}\ , \tag{5}$$

where $E_i=E_g-E_D$ is the ionization energy of donors and N_C is the conduction-band density of states (for GaAs, $N_C=8.36\times10^{13}T^{3/2}$ cm^{-3}).

We fit the experimentally observed $\tau^{-1}(T)$ by using a linear combination of all the scattering rates [Eq. (3)]. The contribution of each of the electron-scattering mechanisms to the total fitting is demonstrated in Fig. 6 for sample B. The fitting curves for all three samples under study are shown in Fig. 2. All three demonstrate very good agreement between the experimental data and the model calculations. From this fitting procedure, the interaction coefficients and other parameters (appearing in Table I) are obtained. The parameters determined from the fitting for sample B were used without change in the fitting procedure for the other samples. These values are in good agreement with the theoretical predictions for the acoustic-phonon piezoelectric scattering and for the acoustic-phonon deformation-potential scattering (see Table I).

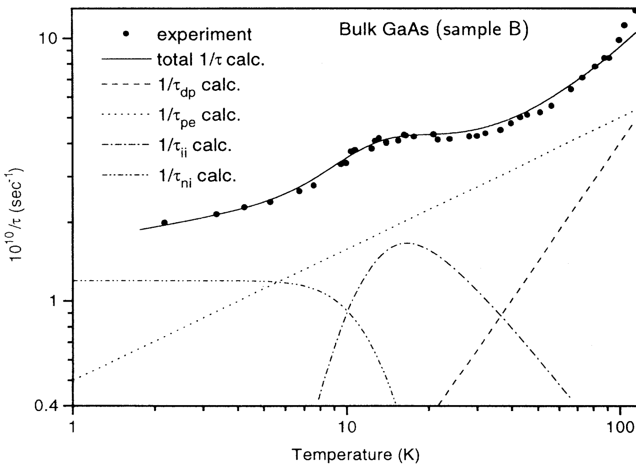

FIG. 6. The temperature dependence of each scattering rate given in Table I with parameters corresponding to sample B. Also shown are the experimental scattering rate and the total model fitting using Eq. (3) for the same sample.

The donor concentration for each of the samples was estimated from the calculated contribution of ionized-impurity scattering to the fitted $\tau^{-1}(T)$ in the temperature range 10–20 K. The concentration values, taking $E_i=5.8$ meV,[3] are given in Table I. Then, these N_D values are used in order to determine the coefficient a in Erginsoy's formula, using the τ_{ni}^{-1} value obtained from the fitting procedure. This derived value of a is different for each one of the samples and exceeds slightly that given by Erginsoy's formula (cf. Table I). The discrepancy may be explained, on the one hand, by a low degree of compensation in our samples, which is not taken into account here, or, on the other hand, by the theoretical prediction[2] that Erginsoy's formula is not fully applicable to compound semiconductors.

The estimated trend of the impurity concentrations obtained from the CR measurements is consistent with the experimental PL spectra (Fig. 4). The PL spectrum of sample A displays a most intense PL line that is due to the exciton polaritons (X). In sample B, the donor-bound exciton PL intensity exceeds that of the free exciton. The exciton lines in sample C are much broader. The absence of an acceptor-bound exciton line for samples A and B shows that they have a very low compensation level.

Consider now the effect of free-electron heating by the MW field on the electron-scattering mechanisms. As $P_{\rm MW}$ increases, the free-electron energy increases so that $T_e>T$.[11] Figure 3 shows that the CR linewidth decreases initially with $P_{\rm MW}$ and then increases. Under high $P_{\rm MW}$, a distortion of the CR line shape is observed along with the line broadening. At $T=2$ K, the only electron-scattering processes are those due to neutral impurities and acoustic phonons via the piezoelectric potential. For example, for the purest A sample, these contributions are approximately equal. Under electron heating, the neutral-impurity-scattering rate remains unchanged while that due to the acoustic-phonon piezoelectric scattering decreases as $T_e^{-1/2}$ (cf. Table I). Consequently, we expect a decrease of the total scattering rate $\tau^{-1}(T)$ approximately to the neutral-impurity-scattering limit. Still at higher $P_{\rm MW}$, the CR line shape is affected by various nonlinear electron heating processes that may include impurity ionization (these will be reported elsewhere). In Fig. 2, the CR linewidth narrowing due to electron heating measured for each sample is marked by an arrow (at $T=2$ K). One can see that, indeed, $\tau^{-1}(T)$ approaches the predicted neutral-impurity-limit value. Note that the $P_{\rm MW}$ range wherein the CR line narrowing occurs is shifted to a higher power for the samples with larger impurity concentrations, namely, from 1 μW for sample A to 10 μW for sample C (Fig. 3). This is a result of the higher MW absorption rate in the sample with the higher mobility (A).

Our experimental ODCR results show that the momentum relaxation rate, extracted from the ODCR

linewidth, appears to be much larger than that deduced from the CR line shape, for the same P_{MW} and I_L (Fig. 5). There is a basic difference between the CR and ODCR methods: ODCR results from the hot electron temperature dependence on the magnetic-field strength and the hot electron effect on the recombination processes. Since the PL intensity is not proportional to the electron temperature,[17] and, moreover, the mobility value cannot be extracted from the dependence $T_e(B)$,[18] the ODCR line shape does not provide a reliable estimate of the carrier mobility [and hence of the $\tau^{-1}(T)$].

Finally, the very narrow electron CR line observed at $T=1.6$ K allows us to measure precisely the electron effective mass. For a magnetic field applied along the [001] direction, it is $m^*=(0.0662\pm0.0002)m_0$. This value corresponds to the very bottom of the GaAs conduction band, namely, to a mean electron energy of 0.14 meV.

IV. SUMMARY

So far, the highest electron mobility value was reported for MBE-grown n-GaAs layers, with a peak mobility of $\sim 4\times10^5$ cm^2/V sec obtained at $T=30$ K.[19] Our study of electron-scattering mechanisms shows that the electron mobility in the purest GaAs sample ($N_D=1.5\times10^{13}$ cm^{-3}) increases as the temperature decreases and reaches 2.2×10^6 cm^2/V sec at $T=1.6$ K. From the analysis of $\tau^{-1}(T)$ we found that this experimentally obtained mobility value is only twice less than that expected for the acoustic-phonon piezoelectric scattering limit. In the case of electron heating by the microwave field, when the electron scattering via the acoustic-phonon piezoelectric potential is greatly reduced (cf. Table I), the measured mobility value increases up to 4.2×10^6 cm^2/V sec. Thus, we find that, in the ultrapure GaAs crystals studied here, the acoustic-phonon piezoelectric scattering is the most significant process even for $T<10$ K.

The difficulty to reach high electron mobility in GaAs is due to the high efficiency of impurity scattering relative to the various phonon-assisted scattering mechanisms. Unlike the well-studied bulk Ge and Si crystals, where the electron-phonon scattering (due to the acoustic deformation potential) dominates even down to $T\sim2$ K (at $N_D\sim10^{14}$ cm^{-3}), the relative contribution of electron-impurity scattering to the mobility in GaAs is higher than that in Ge and Si by ~100. This is a result of the low value of the electron effective mass in GaAs. Therefore, the electron-impurity scattering is significant for $T<30$ K even in high-quality samples and it was believed that the electron-phonon scattering mechanisms could not be studied experimentally in the low-temperature limit.[8]

In conclusion, we presented a detailed study of the classical electron cyclotron resonance and the temperature dependence of the electron momentum relaxation rate $\tau^{-1}(T)$ in ultrapure GaAs crystals. The results were analyzed by a combination of the various mechanisms of electron scattering. From the fit of $\tau^{-1}(T)$, the electron-acoustic phonon interaction parameters as well as the impurity concentrations were obtained. It was found that the electron scattering by acoustic-phonon piezoelectric potential is the main momentum relaxation mechanism in the purest samples at low temperatures. The CR line shape narrowing resulting from free-electron heating by the MW field is explained by the decrease of the acoustic-phonon piezoelectric scattering with electron energy when the momentum relaxation rate decreases down to the neutral-impurity-scattering limit. It is shown that, unlike the CR measurements, the ODCR line shape does not provide a reliable estimate of the carrier mobility value.

ACKNOWLEDGMENTS

We would like to thank Dr. V. V. Bel'kov and Dr. V. V. Rossin of the A. F. Ioffe Institute (St. Petersburg, Russia) for their participation in the first stage of this study and to Dr. V. Umansky of the Weizmann Institute (Rehovot, Israel) for supplying us with the MBE-grown samples. The research at Technion was done in the Barbara and Norman Seiden Center for Advanced Optoelectronics. B.M.A. acknowledges the support of Fondation Rich (France) and the Alexander Goldberg Fund of the Technion.

[1]T. Ohyama, K. Murase, and E. Otsuka, J. Phys. Soc. Jpn. **29**, 912 (1970).

[2]E. Otsuka, Jpn. J. Appl. Phys. **25**, 303 (1986).

[3]T. Ohyama, H. Kobori, and E. Otsuka, Jpn. J. Appl. Phys. **25**, 1518 (1986).

[4]V. K. Arora and H. N. Spector, Phys. Status Solidi B **94**, 701 (1979).

[5]Yu. V. Zhilyaev, G. R. Markaryan, V.V. Rossin, T. V. Rossina, and V. V. Travnikov, Fiz. Tverd. Tela (Leningrad) **28**, 2688 (1986) [Sov. Phys. Solid State **28**, 1506 (1986)].

[6]V. V. Rossin and B. M. Ashkinadze, in *Proceedings of the 22nd International Conference on the Physics of Semiconductors*, edited by D. J. Lockwood (World Scientific, Singapore, 1994), p. 337.

[7]B. M. Ashkinadze, V. V. Bel'kov, and A. G. Krasinskaya, Fiz. Tekh. Poluprovodn. **24**, 572 (1990) [Sov. Phys. Semicond. **24**, 361 (1990)].

[8]K. Seeger, *Semiconductor Physics* (Springer-Verlag, Wien, 1973), Chap. 11.

[9]M. Godlewski, W. M. Chen, and B. Monemar, Crit. Rev. Solid State Mater. Sci. **19**, 241 (1994).

[10]S. Adachi, *GaAs and Related Materials: Bulk Semiconducting and Superlattice Properties* (World Scientific, Singapore, 1994), Chap. 14.

[11]E. M. Conwell, in *High Field Transport in Semiconductors*, edited by F. Seitz, D. Turnbull, and H. Ehrenreich, Solid State Physics Suppl. 9 (Academic, New York, 1967).

[12]H. J. G. Meijer and D. Polder, Physica **19**, 255 (1953).

[13]C. M. Wolfe, G. E. Stillman, and W. T. Lindley, J. Appl. Phys. **41**, 3088 (1980).

[14]V. M. Bright and W. D. Hunt, J. Appl. Phys. **68**, 1985 (1990).

[15]The scattering of electrons by ionized impurities is usually described either by the Brooks-Herring equation [H. Brooks, Adv. Electron. Electron Phys. **7**, 158 (1955)] or by the Conwell-Weisskopf equation [E. Conwell and V. F. Weisskopf, Phys. Rev. **77**, 388 (1950)]. Since these equations give almost the same values of electron mobilities for impurity concentrations up to 10^{18} cm^{-3} (Ref. 8), we have restricted ourselves to the Conwell-Weisskopf expression, where the logarithmic term is due to the ionized-impurity screening by the free carriers.

[16]P. S. Kireev, *Semiconductor Physics* (Mir, Moscow, 1974), Chap. 3.

[17]B. M. Ashkinadze, V. V. Bel'kov, and A. G. Krasinskaya, Fiz. Tekh. Poluprovodn. **24**, 883 (1990) [Sov. Phys. Semicond. **24**, 555 (1990)].

[18]E. Hanamura and T. Inui, J. Phys. Soc. Jpn. **17**, 666 (1962).

[19]C. R. Stanley, M. C. Holland, A. H. Kean, J. M. Chamberlain, R. T. Grimes, and M. B. Stanaway, J. Cryst. Growth **111**, 14 (1991).